Surrogate Model Based on the POD Combined With the RBF Interpolation of Nonlinear Magnetostatic FE Model

T. Henneron, A. Pierquin, S. Clenet

Surrogate Model based on the POD combined with the RBF Interpolation of Nonlinear Magnetostatic FE model

T. Henneron[1], A. Pierquin[1] and S. Clénet[1]
[1]Univ. Lille, Centrale Lille, Arts et Metiers ParisTech, HEI, EA 2697 - L2EP, F-59000 Lille, France

The Proper Orthogonal Decomposition (POD) is an interesting approach to compress into a reduced basis numerous solutions obtained from a parametrized Finite Element (FE) model. In order to obtain a fast approximation of a FE solution, the POD can be combined with an interpolation method based on Radial Basis Functions (RBF) to interpolate the coordinates of the solution into the reduced basis. In this paper, this POD-RBF approach is applied to a nonlinear magnetostatic problem and is used with a single phase transformer and a three-phase inductance.

***Index Terms*—Nonlinear magnetostatic problem, Model Order Reduction, Proper Orthogonal Decomposition, Radial Basis Functions.**

I. Introduction

THE FE method is commonly used to study low frequency electromagnetic devices. This approach gives accurate results but requires large computational times due to numerical or physical features such as a high number of Degrees of Freedom (DoF) in space and also a high number of time steps or the nonlinear behavior of ferromagnetic materials for example. In order to reduce the computational time especially for parametrized model, model order reduction methods have been proposed in the litterature. One of the most popular approach is the POD approach. Based on the solutions of the FE model for different values of parameters (called snapshots), the POD enables to approximate the solution of the FE model in a reduced basis [1]. Then, the initial FE system is projected onto a reduced basis, decreasing the order of the numerical model to be solved for new parameter values. Another approach consists in constructing a metamodel to interpolate directly the solution expressed into a reduced basis for new parameter values. Different approaches can be used, as for example, based on an optimization process [2] or polynomial functions [3]. The RBF interpolation method can be also applied in this context. In the litterature, the POD-RBF approach has been developed for mechanical or thermal problems [4][5] for example.

In this paper, we propose to use a POD-RBF approach in order to build a fast model of the solution of a nonlinear magnetostatic problem. First, the numerical model of nonlinear magnetostatic problem is brieflty presented. Secondly, the POD-RBF approach is developed. Finally, a single phase EI transformer and a three-phase inductance are studied.

II. Nonlinear magnetostatic problem

Let's consider a domain composed with N_{st} stranded inductors, each supplied by a current i_j and a nonlinear magnetic subdomain. To solve the nonlinear magnetostatic problem, the vector potential formulation is used. Then, the strong formulation is

$$\mathbf{curl}(\nu(\mathbf{B})\mathbf{curlA}) = \sum_{j=1}^{N_{st}} \mathbf{N}_j i_j \tag{1}$$

with ν the magnetic reluctivity depending on the magnetic flux density $\mathbf{B}$, $\mathbf{A}$ the vector potential defined by $\mathbf{B} = \mathbf{curlA}$ and $\mathbf{N}_j$ the unit current density of the j^{th} stranded inductor. By applying the FE method, the equation system to solve for $i_j \in I_j$ is

$$\mathbf{M}(\mathbf{X})\mathbf{X} = \sum_{j=1}^{N_{st}} \mathbf{F}_j i_j \tag{2}$$

with $\mathbf{M}(\mathbf{X})$ the curl-curl matrix, $\mathbf{F}_j$ the source vector associated with the j^{th} inductor and $\mathbf{X} \in \mathbf{R}^{N_x}$ the vector of components of $\mathbf{A}$. For 3D problems, the potential $\mathbf{A}$ is discretized on the edge elements. For each inductor j, the magnetic linkage flux can be expressed by $\Phi_j = \mathbf{F}_j^t \mathbf{X}$.

III. Surrogate model based on POD combined with RBF interpolation

From a set of solutions obtained from the evaluation of the FE model (2), called snapshots, for different values of current, a surrogate model is build in order to approximate the solution for any current values. Then, the Proper Orthogonal Decomposition method is combined with the Radial Basis Function interpolation approach. In the following, two inductors are considered to present the approach and the parameter set (i_1, i_2) is denoted by $\mathbf{i} = (i_1, i_2)$. Then, we seek for an approximation $\mathbf{X}_{ap}(\mathbf{i})$ of $\mathbf{X}(\mathbf{i})$ under the form

$$\mathbf{X}_{ap}(\mathbf{i}) = \sum_{l=1}^{M} \psi_l g_l(\mathbf{i}) \tag{3}$$

with $\psi_l \in \mathbf{R}^{N_x}$ components of the reduced basis, so called modes, $g_l(\mathbf{i})$ a scalar function and M the size of the reduced basis, so called number of modes.

A. Reduction of the dimension by POD

From P snapshots $\mathbf{X}_j = \mathbf{X}(\mathbf{i}_j)$, $j = 1, ..., P$, computed for different values of $\mathbf{i}$, the vectors ψ_l, $l = 1, ..., M$, are deduced. The snapshots matrix is defined such as $\mathbf{M}_X = [\mathbf{X}_1, \mathbf{X}_2, ..., \mathbf{X}_P]$. The Singular Value Decomposition (SVD) is applied to $\mathbf{M}_X$, such as $\mathbf{M}_X = \mathbf{USV^t}$ with $\mathbf{U}_{N_x \times N_x}$

and $\mathbf{V}_{P\times P}$ orthogonal matrices and $\mathbf{S}_{N_x\times P}$ the rectangular diagonal matrix of the singular values ranked in a decreasing order. This decomposition allows to obtain a reduced basis $\Psi = [\psi_l, \psi_2, ..., \psi_M]$ of size $N_x \times M$ which corresponds to the M first columns of $\mathbf{U}$. The truncation of the first columns can be determined by taking the M most significative singular values of $\mathbf{S}$. Then, the solution vector $\mathbf{X}$ can be approximated by $\mathbf{X}_{pod}$ under the form

$$\mathbf{X} \approx \mathbf{X}_{pod} = \Psi\mathbf{G} \tag{4}$$

with $\mathbf{G}$ the vector of components of the solution into the reduced basis.

B. RBF interpolation approach

The RBF interpolation approach is used for the determination of scalar functions $g_l(\mathbf{i})$ for $l = 1, ..., M$. From the SVD of $\mathbf{M}_X$, we can deduce the matrix expressed in the reduced basis such as $\mathbf{M}_G = [\mathbf{G}_1, \mathbf{G}_2, ..., \mathbf{G}_P] = \mathbf{S}_{(1:M,1:M)}\mathbf{V}^t_{(1:P,1:M)}$. Then, each line of $\mathbf{M}_G$ corresponds to the discrete values of $g_l(\mathbf{i}_j) = G_{jl}$ for $j = 1, ..., P$. In fact, $g_l(\mathbf{i}_j)$ represents the l^{th} coordinate of the approximation of $\mathbf{X}_j$ in the reduced basis. From these values, the RBF interpolation is performed in order to determine each function $g_l(\mathbf{i})$ under the following form

$$g_l(\mathbf{i}) = \sum_{j=1}^{P} \alpha_{lj}\phi_j(\mathbf{i}) \tag{5}$$

with $\phi_j = \phi(||\mathbf{i} - \mathbf{i}_j||)$ a radial function depending on the Euclidian distance between $\mathbf{i}$ and $\mathbf{i}_j$ and α_{lj} its associated coefficient. The coefficients α_{lj} are calculated to interpolate the P vectors $\mathbf{G}_k$

$$G_{kl} = g_l(\mathbf{i}_k) = \sum_{j=1}^{P} \alpha_{lj}\phi_k(||\mathbf{i}_k - \mathbf{i}_j||) \quad \text{for } k = 1, .., P. \tag{6}$$

Then, we can define an equation system for the computation of the coefficients α_{lj}, $j = 1, ..., P$, such as

$$\begin{aligned} &\mathbf{Y}_l = \mathbf{B}\mathbf{A}_l \\ &\text{with } \mathbf{Y}_l = [G_{1l}, ..., G_{Pl}]^t, \mathbf{A}_l = [\alpha_{l1}, ..., \alpha_{lP}]^t \\ &\text{and } \mathbf{B} = \begin{bmatrix} \phi_1(\mathbf{i}_1) & \cdots & \phi_1(\mathbf{i}_P) \\ \vdots & \ddots & \vdots \\ \phi_P(\mathbf{i}_1) & \cdots & \phi_P(\mathbf{i}_P) \end{bmatrix}. \end{aligned} \tag{7}$$

The number of equation system (7) to solve depends on the number of modes M (i.e. the size of the reduced basis). The error of interpolation depends on the choice for the radial function. Table I presents different examples of function where a is a parameter fixed by the user, called "shape parameter". Finally, for any coordinate $\mathbf{i}_{new}$, we can compute an approximation $\mathbf{X}_{ap}(\mathbf{i}_{new})$ of the FE solution by (3).

C. Greedy algorithm

In order to optimize the size of the reduced basis Ψ and the number of snapshots used for the interpolation, a greedy algorithm can be applied. In this case, Q snapshots of the FE model (2) are computed, the aim of the greedy algorithm is to select the most significant P vectors $\mathbf{X}$ among the Q snapshots to build the POD-RBF model in order to reduce the memory requirements, i.e. the number of coefficents α_{lj} and the size of the reduced basis. We denote $\mathbf{p}_k$ a coordinate among $\mathbf{i}_j$ for $j = 1, ..., Q$, the vector of coordinates selected by the greedy algorithm is $\mathbf{p} = [\mathbf{p}_1, ..., \mathbf{p}_P]$ and ϵ_f is a criterion fixed by the user to stop the iterative algorithm.

TABLE I
EXAMPLES OF RBF FUNCTION

Name	$\phi(\mathbf{x})$
Gaussian (G)	$e^{-(\mathbf{x}/a)^2}$
Multiquadric (MQ)	$\sqrt{1+(\mathbf{x}/a)^2}$
Inverse multiquadric (IMQ)	$\sqrt{\frac{1}{1+(\mathbf{x}/a)^2}}$
Thin plate spline	$\mathbf{x}^2 log(\mathbf{x})$

Algorithm 1 Greedy algorithm

Input: $\mathbf{M}_X = [\mathbf{X}(\mathbf{i}_1), \mathbf{X}(\mathbf{i}_2), ..., \mathbf{X}(\mathbf{i}_Q)]$, $\mathbf{p}_1$
Output: M, P, Ψ and α_{lj}

- $P = 0$
while $\epsilon_X > \epsilon_f$ **do**
  - $P = P + 1$
  if $P > 1$ **then**
    - select the coordinate corresponding to the maximum of the error such as $\mathbf{p}_P = argmax(\mathbf{e})$
  end if
  - $\mathbf{p} \leftarrow [\mathbf{p}, \mathbf{p}_P]$
  - $\mathbf{M}_S \leftarrow [\mathbf{M}_S, \mathbf{X}(\mathbf{p}_P)]$
  - from $\mathbf{M}_S$, update Ψ and the coefficients α_{lj}
  - compute the vector $\mathbf{e}$ of the norm of relative errors such as $\mathbf{e} = [e_k]_{k=1}^{Q}$ with $e_k = \frac{||\mathbf{X}(\mathbf{i}_k) - \mathbf{X}_{ap}(\mathbf{i}_k)||_2}{||\mathbf{X}(\mathbf{i}_k)||_2}$
  - compute the average of the errors $\epsilon_X = \frac{1}{Q}\sum_{k=1}^{Q} e_k$.
end while

The average error of the magnetic linkage flux for the j^{th} inductor can be also defined such as

$$\epsilon_{\Phi_j} = \frac{1}{Q}\sum_{k=1}^{Q} e_{\Phi_{j,k}} \text{ with } e_{\Phi_{j,k}} = \frac{|\Phi_j(\mathbf{i}_k) - \Phi_{ap,j}(\mathbf{i}_k)|}{|\Phi(\mathbf{i}_k)|}. \tag{8}$$

IV. APPLICATION

Two examples of application are studied. The first one is a single phase transformer and the second one is a three-phase inductance.

A. Single phase transformer

Due to the symmetries, only one eighth of the single phase EI transformer is modeled. Figure (1) presents the mesh of the magnetic core and of the windings (a) and the nonlinear $B(H)$ magnetic curve (b). The 3D mesh is composed of 67177 tetrahedron elements, the number of DoF is $N_x = 76663$. The FE model (2) is solved $Q = 225$ times with 15 equidistributed values N_{i_1} for $i_1 \in [0 : 1]A$ and N_{i_2} for $i_2 \in [-2 : 0]A$. In these conditions, the computational time is $135min$ (all

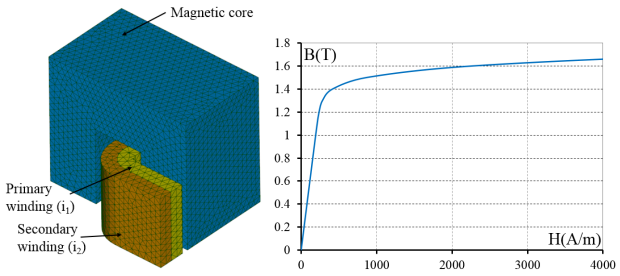

(a) Mesh (b) Non-linear curve

Fig. 1. Single phase EI transformer.

computations have been achieved with an Intel Xeon Processor E5-2690 v3, 3.5GHz, 256Go RAM).

In order to evaluate the influence of the parameters of the RBF interpolation method, we propose to study the evolution of the error ϵ_X versus the number P of solutions selected by the greedy algorithm for different type of radial functions and for different values of the shape parameter. Figure (2) presents the errors for three different radial functions (G, MQ and IMQ see Table I) with a shape parameter $a = 0.1$. The best convergence is obtained with the multiquadric (MQ) functions. However when P becomes large, the gaps between the errors obtained with the three RBF decrease. Figures (3) and (4) present the errors for the IMQ and MQ functions with different values of the shape parameter a. With the IMQ functions, the convergence is influenced by the shape parameter when P is small. For $P = 150$, the different errors are similar. For the MQ functions, no significant difference can be observed on the convergence of the error for the different values a. For the IMQ or G functions, greater a is important, most influential is the approximated solution by snapshots.

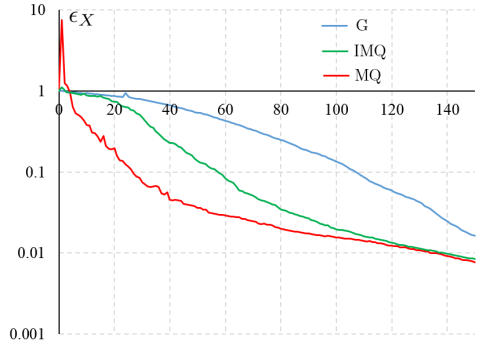

Fig. 2. Errors versus the number P of solutions selected by the greedy algorithm ($a = 0.1$).

Figures (5) and (6) present the magnetic flux density obtained from the POD-RBF model and the difference of $\mathbf{B}$ obtained from the FE model and the POD-RBF approximation for different values of currents not used to compute snaphots. Then, we consider $(i_1 = 0.95A, i_2 = 0A)$ for the first case and $(i_1 = 0.4A, i_2 = -0.9A)$ for the second case, the MQ functions are used for the interpolation with $a = 0.1$ and $P = 150$. For both cases, the magnitudes of the error are very small compared with those of the magnetic flux density. The

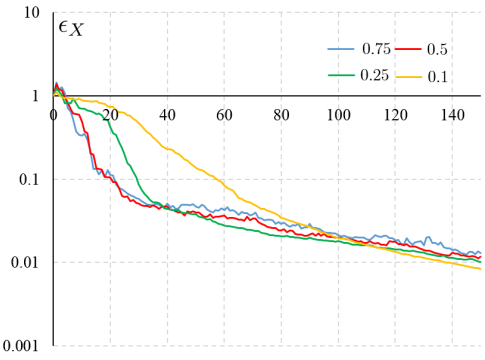

Fig. 3. Errors versus the number P of selected solutions with IMQ functions and for different values of the shape parameter a.

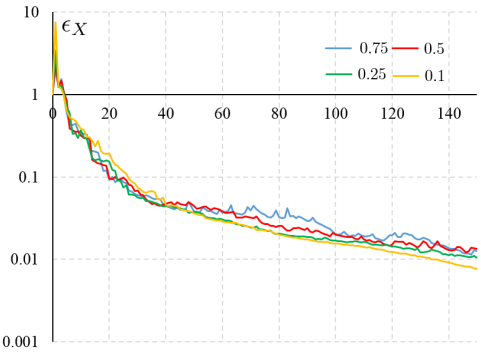

Fig. 4. Errors versus the number P of selected solutions with MQ functions and for different values of the shape parameter a.

maximum of the error is located on the internal corners of the magnetic core where saturation effect is the most prominent.

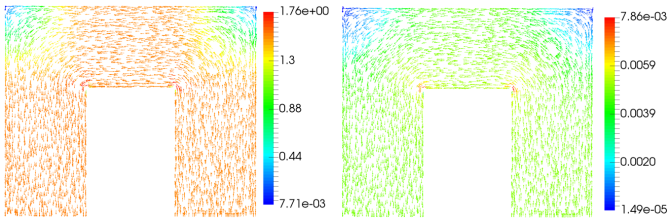

Fig. 5. Magnetic flux density (T) and error on $\mathbf{B}$ for $(i_1 = 0.95A, i_2 = 0A)$.

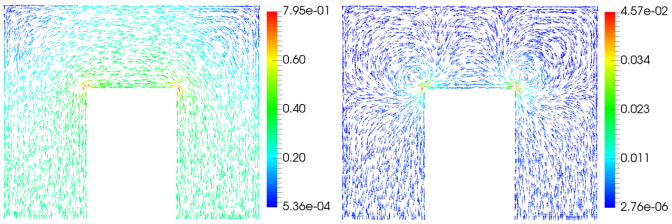

Fig. 6. Magnetic flux density (T) and error on $\mathbf{B}$ for $(i_1 = 0.4A, i_2 = -0.9A)$.

The POD-RBF model gives a compressed form of data from the Q solutions $\mathbf{X}$ of the FE model. The number of terms extracted from the solutions of the FE model is 76663×225. For $P = 150$, the POD-RBF model requires 76663×45 terms to be stored for the reduced basis Ψ and, for the interpolation,

150×45 coefficients α_{lj} and 150×2 for the coordinates $\mathbf{i}$ of the 150 solutions. Then, the compression factor calculated by $1 - \frac{\text{terms of POD-RBF model}}{\text{terms from FE model}}$ is 80% for an error of about 0.8% and a computational time equal to $7min$ for the determination of the POD-RBF model. If a coarse surrogate model with an acceptable error about 5% is sufficient for a study. Then, the compression factor is 91% and the computational time is about $1min$.

B. Three-phase inductance

Due to the symmetries, one quarter of the three-phase inductance is modeled. Figure (7) presents the mesh of the magnetic core and of the windings. The 3D mesh is composed of 66382 tetrahedron elements, the number of DoF is $N_x = 75584$. The nonlinear curve of the magnetic core presented on Fig. (1-b) is considered. The FE model (2) is solved 2197 times with 13 equidistributed values for N_{i_1}, N_{i_2} and N_{i_3} with the same current interval $I = [-6 : 6]A$ for all currents. In these conditions, the computational time is of $57.7h$.

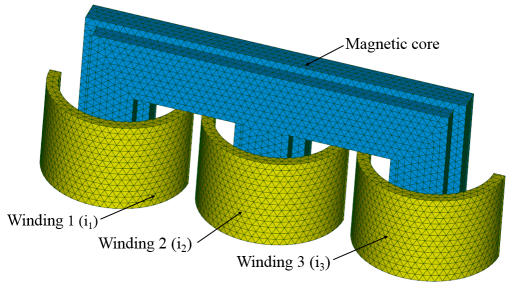

Fig. 7. Mesh of the three-phase inductance.

Figure (8) presents the evolution of the error on the solution and on magnetic linkage fluxes versus the number P of selected solutions when the MQ functions are used for the interpolation with $a = 0.25$. With $P = 500$, the error ϵ_X is close to 1% and the errors ϵ_{ϕ_1}, ϵ_{ϕ_2} and ϵ_{ϕ_3} are about 4%. Then, the computational time is $5h$. The POD-RBF model requires 75584×130 terms to be stored for the reduced basis Ψ, 500×130 coefficients α_{lj} and 500×3 for the coordinates $\mathbf{i}$ of the 500 solutions for the interpolation, which corresponds to a compression factor of 94%.

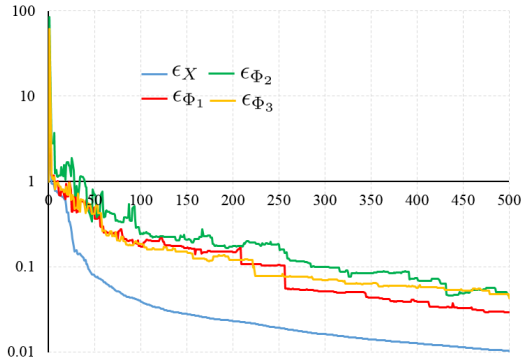

Fig. 8. Errors versus the number P of selected solutions.

Figures (9) and (10) present the magnetic flux density obtained from the POD-RBF approximation and the difference of $\mathbf{B}$ obtained from the FE and POD-RBF models for different values of currents not used for the snaphots. For the first case, we consider $(i_1 = 5.5A, i_2 = -2.75A, i_3 = -2.75A)$ which corresponds to a balanced current supply. For the second case, we consider $(i_1 = 0A, i_2 = 5.75A, i_3 = 0A)$ in order to simulate a single phase EI inductance. For both case, the magnitudes of the error are fully acceptable according to fact that this error is at most of same order of the one introduced by the uncertainties we have on the dimensions and on the behavior law of the materials. The maximum of the error is located on the internal corners of the magnetic core as for the first application example.

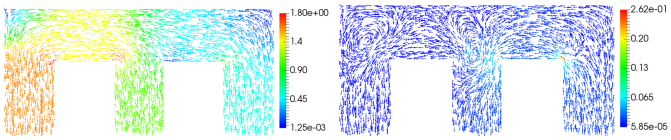

Fig. 9. Magnetic flux density (T) and error on $\mathbf{B}$ for $(i_1 = 5.5A, i_2 = -2.75A, i_3 = -2.75A)$.

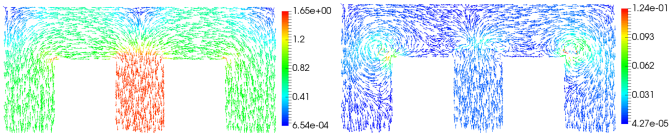

Fig. 10. Magnetic flux density (T) and error on $\mathbf{B}$ for $(i_1 = 0A, i_2 = 5.75A, i_3 = 0A)$.

V. Conclusion

A surrogate model based on the POD combined with the RBF interpolation approach of a nonlinear magnetostatic FE model has been developed. From the examples of application, this approach enables to obtain an approximation of the FE solution with reasonable computional times and a good accuracy. In this context, the POD-RBF model could be coupled with electrical equations in order to simulate a non linear magnetostatic device in its environment.

References

[1] J. Lumley, 'The structure of inhomogeneous turbulence', *Atmospheric Turbulence and Wave Propagation*, A.M. Yaglom and V.I. Tatarski., pp. 221-227, 1967.

[2] R.R. Rama, S. Skatulla, C. Sansour, "Real-time modelling of the heart using the proper orthogonal decomposition with interpolation", VI International Conference on Computational Bioengineering, ICCB 2015, 2015.

[3] M. Farzam Far, F. Martin, A. Belahcen, L. Montier, T. Henneron, "Orthogonal Interpolation Method for Order Reduction of a Synchronous Machine Model," *IEEE Trans. Mag.*, vol. 54(2), pp. 1-6, 2018.

[4] W.P. Adamczyk , Z. Ostrowski, Z. Buli?ski, A. Ryfa, "Application of POD-RBF technique for retrieving thermal diffusivity of anisotropic material", 9th International Conference on Inverse Problems in Engineering, 2017.

[5] V. Buljak, "Proper orthogonal decomposition and radial basis functions algorithm for diagnostic procedure based on inverse analysis", *FME Transaction*, vol. 38, 2010.